IJIE

The International Journal of Integrated Engineering

Cutting Force and Surface Roughness Optimizations in End Milling of GFRP Composites Utilizing BPNN-Firefly Method

M. Khoirul Effendi[1*], Bobby O. P. Soepangkat[1], Rachmadi Noorcahyo[2], Suhardjono[1], Sampurno[1]

[1]Mechanical Engineering Department, Institut Teknologi Sepuluh Nopember, Kampus ITS Sukolilo, Surabaya, 60111, INDONESIA

[2]Mechanical Engineering Department
Universitas Gajah Mada, Jl. Yacaranda Sekip unit IV, Blimbing Sari, Caturtunggal, Kec. Depok, Kabupaten Sleman, Daerah Istimewa Yogyakarta, 55281, INDONESIA

*Corresponding Author

Abstract: The excessive cutting force that is generated in the end milling process of glass fiber-reinforced polymer (GFRP) composites can lower the surface quality. Hence, it is necessary to select the correct levels of end milling parameters to minimize the cutting force (CF) and surface roughness (SR). The parameters of the end milling process comprised the depth of cut (doc), spindle speed (n), and feeding speed (V_f). This study emphasized on the modeling and minimization of both CF and SR in the end milling of GFRP combo fabric by combining backpropagation neural network (BPNN) method and firefly algorithm (FA). The FA based BPNN was first performed to model the end-milling process and predict CF and SR. It was later also executed to obtain the best combination of end-milling parameter levels that would provide minimum CF and SR. The outcome of the confirmation experiments disclosed that the integration of BPNN and FA managed to accurately predict and substantially enhance the multi-objective characteristics.

Keywords: BPNN, cutting force, end milling, firefly algorithm, GFRP, optimization, surface roughness

1. Introduction

Glass fiber-reinforced polymer (GFRP) composites are commonly used in industrial sectors, such as aerospace, marine, aviation, automotive, electronics, and many others. They have extraordinary material properties on the specific stiffness, fracture toughness, strength to weight ratio, impact resistance, and lightweight. Furthermore, most GFRP-composite-based products are shaped during the cycle of the curing process. This later requires accuracy of the dimension during the assembly of the final product during the machining processes [1]. With regards to that, a composite material removal operation process called end milling is suggested to be utilized. The process is considerably applicable in various manufacturing industries, such as automotive and aerospace, for removing excess materials and producing high-quality surfaces used to join the composite materials. GFRP composites consist of glass as the filler and polymer as the matrix. This particular type of composites is usually inhomogeneous as well as having anisotropic properties and abrasive behavior. For this reason, the end milling process would substantially be affected by the catastrophic nature of the composite characteristics [2, 3]. Next, during the end milling process, there is still a possibility that processing the GFRP composites to fail due to the emergence of unoptimized machining forces that would potentially increase the surface roughness level. To prevent this to occur, it is necessary to specify the correct levels of end milling variables in order to minimize the CF and SR through performing necessary optimizations [4].

Machining force and surface roughness are quality attributes which are considered to be directly contributing to the end milling processing of GFRP composites [5-8]. Also, spindle speed, feeding speed, and depth of cut are the three parameters involved in the process. In this case, they are influential in determining the machining force and surface roughness; this is supported by the four previously mentioned references.

Selecting the right combination of parameters with simultaneously multiple specifications through experimentations is considered costly, time-consuming, and tedious. Therefore, researchers have applied soft computing techniques to conduct process parameter optimizations of machining. Soft computing techniques have gained popularity among researchers since they are able to help solve highly complicated problems such as nonlinear, multidimensional, and challenging engineering problems [9]. These techniques consist of algorithms and techniques to find possible solutions for specific or complex problems and propose the best solution. Moreover, soft computing techniques also acknowledge the uncertainty and imprecision variable in completing the processes.

In particular, a swarm intelligence algorithm called firefly has been used to optimize machining areas and solve continuous and discrete problems in machining processes. A number of articles have reported the success of single and multi-objective optimizations using two responses using the firefly algorithm (henceforth FA) in the turning process [10], [11], [12], [13], and laser cutting [14]. Nevertheless, the literature survey reveals that there were not any publications on the multi-objective simultaneous optimization of cutting force and surface roughness using the FA in the end milling process of GFRP. In this study, a backpropagation neural network (henceforth BPNN) model was established to predict the effect of the end milling process parameters on cutting force and surface roughness. Then, an optimal number of hidden nodes applied in this model was identified by incorporating the FA with the BPNN. The FA was then embedded into the neural network model to obtain optimum operating parameters for the end-milling of GFRP composites.

2. Research Methodology

2.1 Backpropagation Neural Network

BPNN is an artificial neural network (ANN) technique proposed by Rumelhart et al. [15] that offers a supervised learning procedure to model complicated linear and nonlinear systems by matching the output (response data) and input (process parameter data). The basic model of BPNN comprises one input layer, hidden layer, and output layer, with every layer having several connected neurons between the layers. Every neuron in each layer has weight and bias that represent the relationship between the input and output layer. The bias and weight adjustments for each neuron were completed using the error function to reduce the BPNN model training sample error.

The steps of conducting model developments using BPNN are as follows [15, 16]:

Step 1: Normalizing the input and output data from the experimental results within the range of 0 to 2

Step 2: Developing the BPNN architecture, which involves determining the number of hidden layers, number of neurons in the input, hidden, and output layers, initial weight and bias for each neuron, as well as set of training, testing, and data validation, and learning rate

Step 3: Conducting BPNN training

Step 4: Saving the mean of square error (MSE) and checking the stopping criteria

Step 5: Identifying and saving the BPNN architecture with the smallest MSE

Step 6: Saving the BPNN model and objective function

2.2 Firefly Algorithm

FA is a metaheuristic method which was initially established by Yang [17]. This method is commonly used for solving mathematical optimization where the objective function of optimization problem is produced by BPNN topology. The advantages of using FA include the suitability for a non-liner case, fast convergence rate, omission of requirement for a good initial value to start the operation, and ability to detect some local optimum numbers within a single process. In principle, this method adopts flashing patterns and characteristics of fireflies that live in tropical regions. Fireflies are insects of which body produces flickering light through chemical reactions. This light is used to attract other fireflies for reproducing and warn other fireflies about the presence of dangerous predators. The FA's pseudo-code is structured as follows [17]:

Begin
  1) Objective function: $f(x)$
  2) Generate an initial population of fireflies x_i
  3) Formulate light intensity I
  While (t < maximum epoch)
      for $i = 1: n$ (all n fireflies)
          for $j = 1: i$ (n fireflies)
              if ($I_j > I_i$),
                  Updating distance, light intensity and evaluate new solution

```
        end if
      end for j
    end for i
    Rank fireflies and find the current best of optimization
  end while
Display best optimization result
End
```

The attractiveness level of fireflies is contingent upon the brightness level, and distance between two fireflies. In general, fireflies with a dimmer light will move towards fireflies that have a brighter light. If the brightness level is equal, then a firefly will move arbitrarily. In relation to the optimization process, the brightness level of fireflies is manipulated by the objective function of an optimization case. The movement of a firefly (x_i) is influenced by the brightness level of other fireflies (x_j), which is formulated in the following equations [17, 18]:

$$x_i^{t+1}=x_i^t+\beta_0 e^{-\gamma r_{ij}^2}\left(x_j^t-x_i^t\right)+\alpha\epsilon_i^t \tag{1}$$

$$r_{ij}=\left\|x_i^t-x_j^t\right\| \tag{2}$$

Where r_{ij} is the Cartesian distance between firefly i and j, β_0 is the firefly's attractiveness when distance the (r) = 0, α is the random parameter, ϵ_i^t is the random value derived from the Gaussian distribution at time t, γ is the media light absorption coefficient.

Figure 1 shows the procedure for predicting the minimum margin of cutting force (CF) and surface roughness (SR) for GFRP materials during the end milling process under the BPNN method. First, the experimental data were divided into three different groups for training, testing and validation. A normalization process was later used to convert the original value to a specific range for distribution of weights of responses. The BPNN model was then generated to get the smallest MSE value by changing the number of hidden layers, node, and activation function. The FA then employed this model to predict the best value. Finally, denormalization was used to convert the optimization result to its original value.
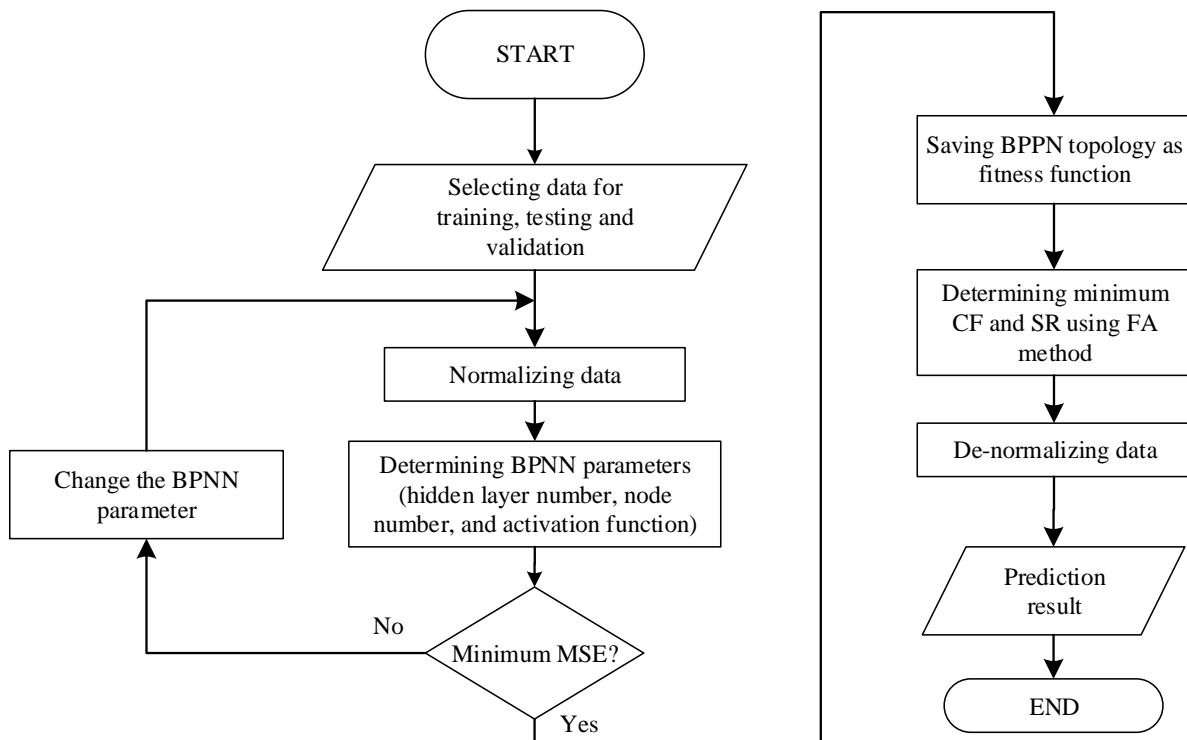

Fig. 1 - Flow chart of CF and SR prediction using BPNN-FA method

3. Experiments and Results
## 3.1 Experimental Setup and Materials

This study used a GFRP material which was produced using the hand lay-up technique and the type of glass fiber was a combo fiber with epoxy as the applied resin. The specimen dimensions were 60 mm (length), 30 mm (width), and 3.7 mm (thickness). Table 1 below summarizes the levels of the variables used in the end milling process. The design for the experiments was a completely randomized factorial design $3 \times 3 \times 3$, with two replications.

Table 1 - End milling process variables

End milling process variables	Unit	Levels		
		1	2	3
Depth of cut (doc)	mm	1	1.5	2
Feeding speed (V_f)	mm/min	500	750	1000
Spindle speed (n)	rpm	3000	4000	5000

The kind of solid carbide tool used in this study for the end milling was YG type K-2 EMC 54060 with 6 mm. Hartford S-Plus 10 vertical milling was used to perform the slotting milling process without any coolant. The number of flutes used was as many as 4. The symbols F_x, F_y, and F_z represented the feed, cutting, and thrust forces, respectively. Next, they were measured using Kistler dynamometer 9272. Figure 2 illustrates this process. Additionally, this particular type of dynamometer was previously used in previous research studies [19, 20, and 21] to measure the value of cutting forces during the face milling process. The resultant cutting force (CF) was calculated using the following formula [4, 21, and 22]:

$$CF = \sqrt{F_x{}^2 + F_y{}^2 + F_z{}^2} \tag{3}$$
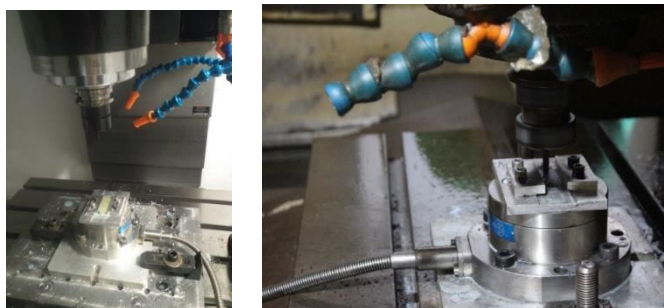
Fig. 2 - The forces measurements in end-milling of GFRP using Kistler 9272 dynamometer

3.2 Experimental Results

Figure 3 and 4 display the measured CF and SR as the combination of doc, n, and V_f. The figures show that the CF and SR value trace a steady path in a wide range of cutting conditions. Also, the depth of cut, spindle speed, and feeding speed were shown to influence both the CF and SR.

4.1 Modeling and Multi-Objective Optimization
4.2 BPNN Model Development

In this study, the process variables involved in the end milling were feeding speed, n, and doc, while the parameter output to be optimized was CF. The variations in the number of hidden layers were between one and five, while the variations in the number of neurons at each layer were between one and ten. The maximum number of epochs was then set as 1000 epochs. Furthermore, the total data (81) was categorized into three groups, where 70%, 15%, and 15% were applied for training, testing, and validation, respectively. Next, satlin, logsig, and tansig activation functions were selected and used in determining the best BPNN topology. The minimum value of MSE was applied to determine the best BPNN topology for two objective functions, namely CF and SR. The optimum BPNN topology was later achieved using a specific number of hidden layers, neurons in each hidden layer, and type of activation-function as presented in Table 2. Figure 5 illustrates the correlation coefficient graphs of CF and SR which were produced by BPNN for training, testing, validation, and all. Since all the correlation coefficient value was close to one, the BPNN output or predicted results were in full correspondence with those from the experimental data. Later, Figure 6 and 7 show the graphical data comparison between the experimental and predicted data responses using BPNN for CF and SR and the average error

margins were 2.77 percent and 4.37 percent. This shows that the prediction result of the end-milling process response is close to the experimental data.
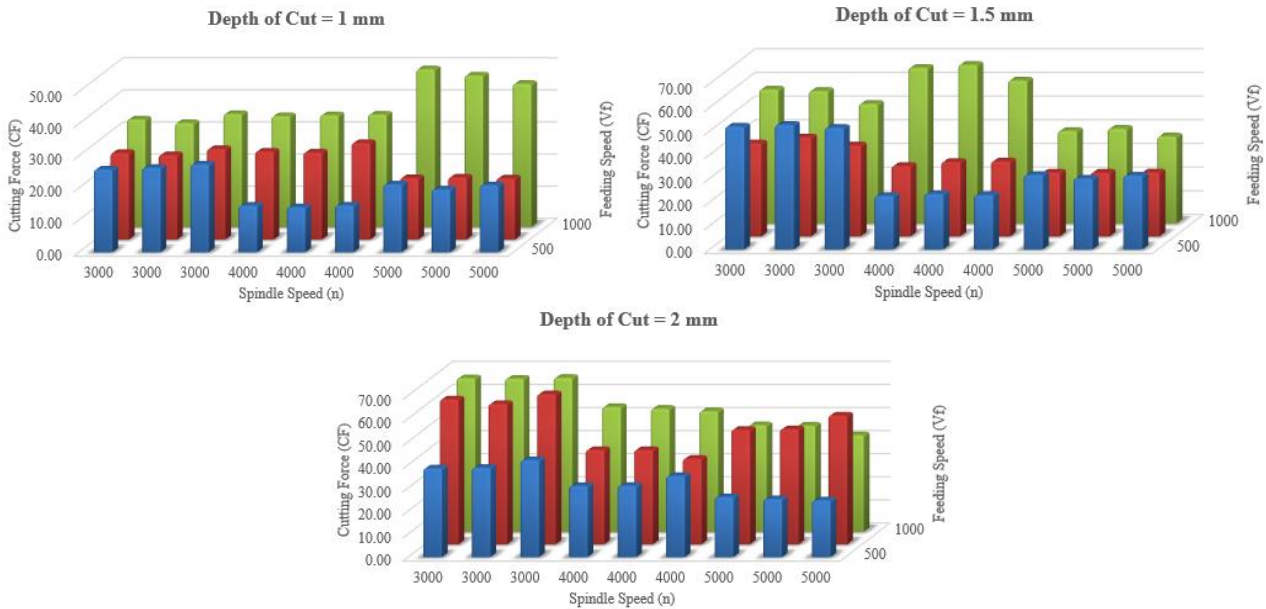

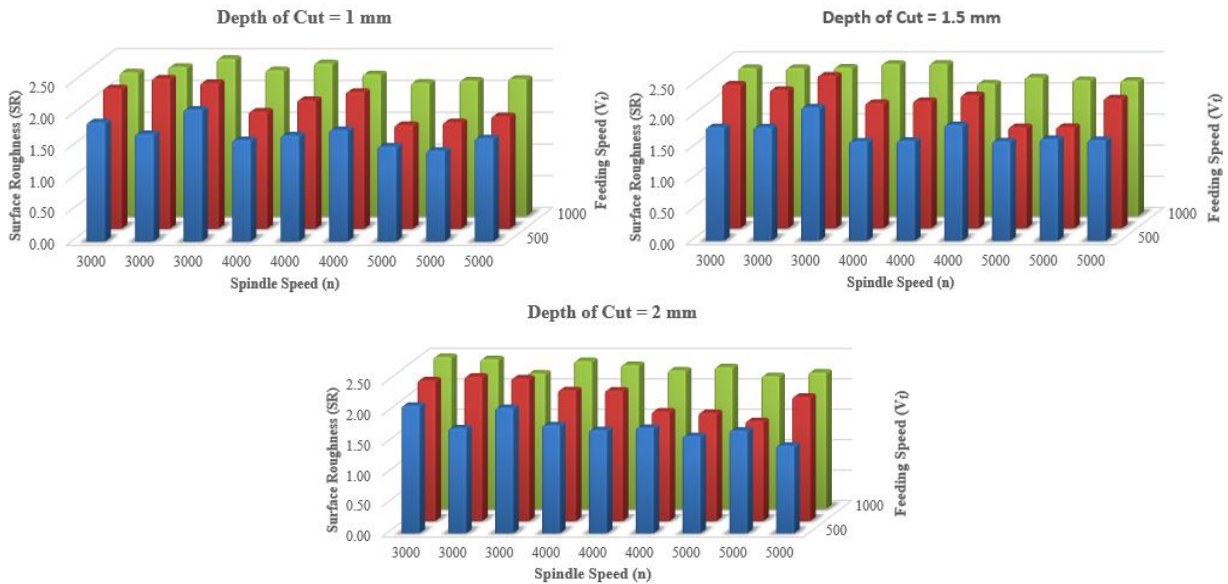**Fig. 3 - Measured CF as the results of the combination of doc, n and V$_f$**

Fig. 4 - Measured SR as the results of the combination of doc, n and V$_f$

Table 2 - Summary of the activation function, MSE values, and optimum BPNN topology of CF and SR

Parameters	BPNN of cutting force	BPNN of surface roughness
Activation function	logsig	satlin
Mean Squared Error (MSE)	0.0030283	0.041197
Number of hidden layers	4	1
Number of neurons each hidden layer	8	8

(a)   (b)
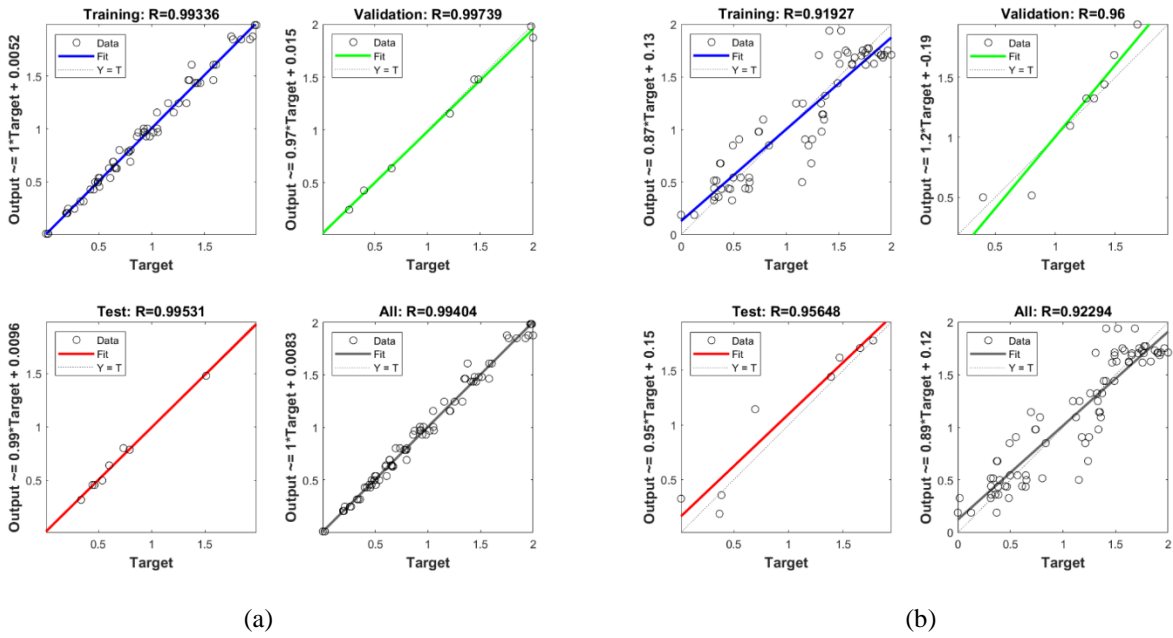
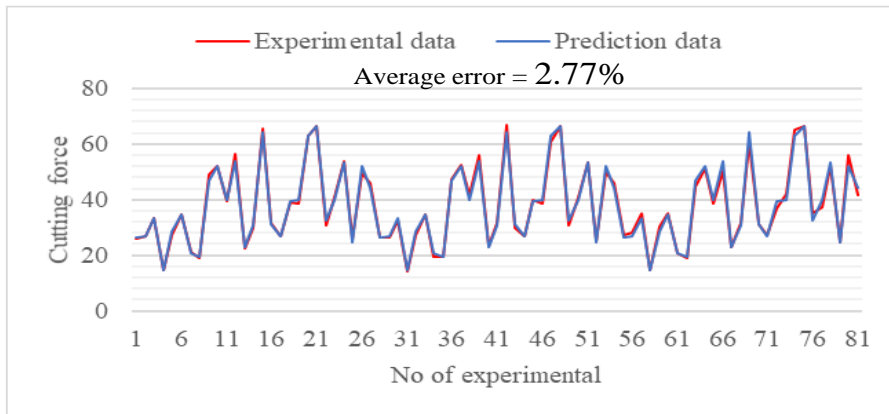**Fig. 5 - Correlation coefficient graphs of BPNN for training, testing, validation, and all for (a) CF and (b) SR**

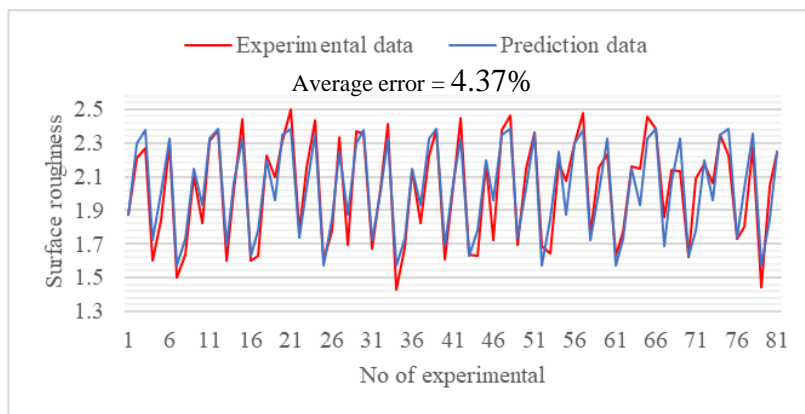**Fig. 6 - The CF value comparison between the experiment and prediction using BPNN**

Fig. 7 - The SR value comparison between the experiment and prediction using BPNN

4.2 Multi-objective Optimization Using FA

For the purpose of coding, the parameter $\beta_0 = 1$, $\alpha = 0.2$, $\gamma = 1$, $\epsilon_i^t = 0.97$, and maximum number of iterations = 50. The fitness function was later obtained from two objective-functions (CF and SR), as shown in the following equation [17, 18]:

$$\min f(x) = w_1 \times Obj_1 + w_2 \times Obj_2$$

(4)

Where:
Obj_1 = objective function of CF obtained using BPNN topology
w_1 = weight of Obj_1 where it is assumed to be 0.5
Obj_2 = objective function of SR obtained by BPNN topology
w_2 = weight of Obj_1 where it is assumed to be 0.5

Figure 8 shows the result of FA algorithm in determining the minimum CF value within 50 iterations, where the optimum fitness value is 0.1248. As the value of CF and SR was 0.5 × the optimum fitness value, the value of CF and SR before denormalization was 0.0624. The levels of the end milling process variables, CF, and SR obtained using FA before and after denormalization can be seen in Table 3. The confirmation experiment using the optimum end-milling parameter setting is then replicated five times. It is later shown that the error value between the BPNN prediction results and confirmation experiment is below 5% for all the responses. This verifies that the value obtained from the prediction of the end-milling process response has an insignificant difference with that from the experimental data.
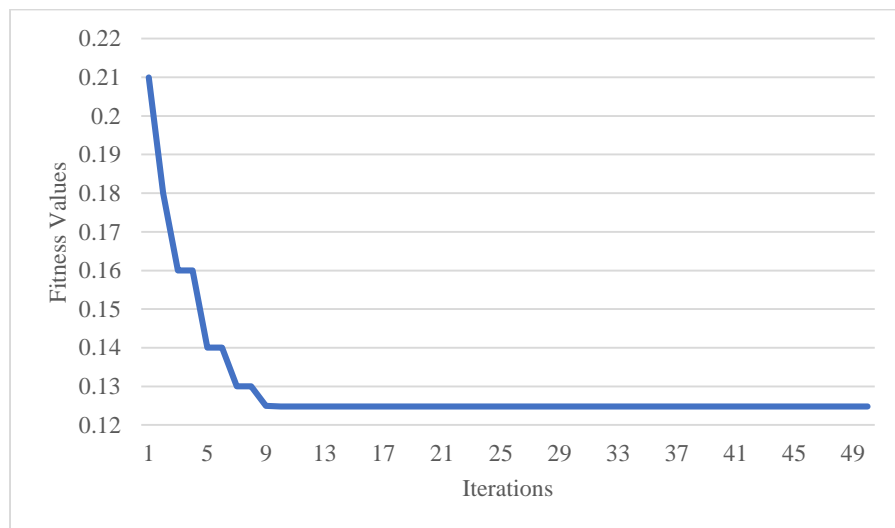

Fig. 8 - Fitness values vs. iterations in determining minimum CF and SR using FA method

Table 3 - The optimum result obtained from the FA method.

End milling process variables	Units	Before denormalization	After denormalization
Depth of cut (doc)	mm	0.0482	1
Spindle speed (n)	rpm	1.4912	4491.2
Feeding speed (V_f)	mm/min	0.4737	618.4
End milling responses	**Units**	**Before denormalization**	**After denormalization**
Cutting force (CF)	N	0.0624	12.4
Surface Roughness (SR)	μm	0.0624	1.4

5. Results and Discussions
5.1 Confirmation Experiments

Through the completion of the multi-response optimization using the BPNN-FA method, the optimum value of CF and SR was obtained by setting the spindle speed, feeding speed, and depth of cut at 4491.2 rpm, 618.4 mm/min, and 1 mm, respectively. This setting of parameters for the process was later functioned as the input to predict the value of

responses through BPNN. The results of comparison between the CF and SR factor and confirmation experiments are presented in the Table 4 below.

**Table 4 - Comparison between BPNN-FA prediction and confirmation experiment**

End milling Parameters			Cutting Force (N)		Surface Roughness (µm)	
Depth of Cut (mm)	Spindle Speed (rpm)	Feeding Speed (mm/min)	Pred./Exp.	Error (%)	Pred./Exp.	Error (%)
1	4491	618	12.4/12.90	3.87	1.4/1.47	4.76

5.2 Effects of the End Milling Variables on Cutting Force and Surface Roughness

Figure 9 displays the influence of process parameters on the value of CF. It shows that the CF increases as the depth of cut increases, and the feeding speed decreases as the spindle speed increases. Various research results have shown that feeding speed is the parameter that most significantly influences the CF response [23, 24, 25, 26]. This can be due to the increase in the feeding speed, which in turn increases the undeformed chip cross-sectional area before the cutting process [4]. Next, the influence of the depth of cut on the CF is shown to be dominant. Increasing the depth of cut will also increase the cross-sectional area and the number of fibers to be cut, which causes the cutting force to increase as well. On the other hand, increasing the spindle speed will decrease the CF response. This happens because the increase in spindle speed will also increase the friction force on the cutting surface. Thus, the temperature on the cutting surface increases. In light of the fact that glass fiber and epoxy resin have low thermal conductivity, the heat on the cutting surface is not well dissipated. As a result, the heat concentrated in the cutting area will cause the matrix around the area to become softer, then the cutting force will decrease. Figure 10 shows the influence of process parameters on SR. It clearly shows that increasing the feeding speed will increase the SR. This may occur due to the increased value of feeding speed which will later increase the strain rate. Later, it causes severe cracks in the glass fiber and epoxy material [4]. The increase in surface roughness is driven by the increased feeding speed, following the theoretical equation for SR; where $Ra = f2/18 (3R)0.5$ [27]. Figure 10 also depicts the phenomenon of the increased rate of the spindle speed that results in the decreased value of the SR. The reason to this to occur is that the increasing value of spindle speed reduces the deformation of tool-chip interface such that the surface becomes smoother. However, it is not suggested that the operator set the spindle speed level to be overly high since the abrasive nature of the GFRP material can result in the premature wear of the tool. Similarly, the results of research studies reported in [4, 23, 24, 25] show the same phenomena, that increasing the spindle speed will decrease the surface roughness. Increasing the depth of cut is said to increase the surface roughness, although the effect is not very significant. The research conducted by [25] and [28] also identified the same results.
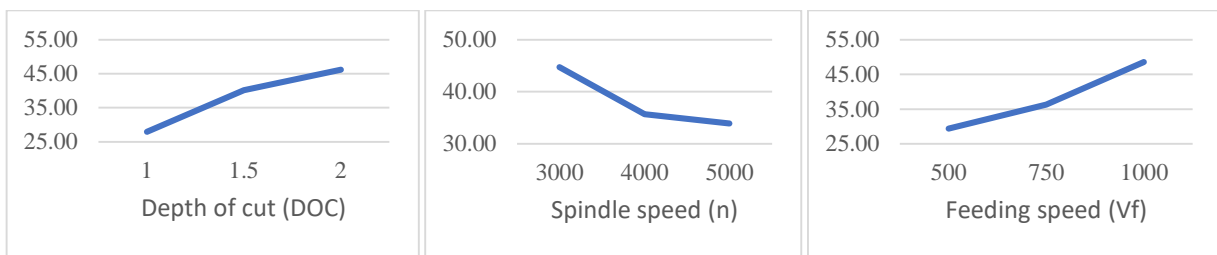
Fig. 9 - The influence of process parameters on CF
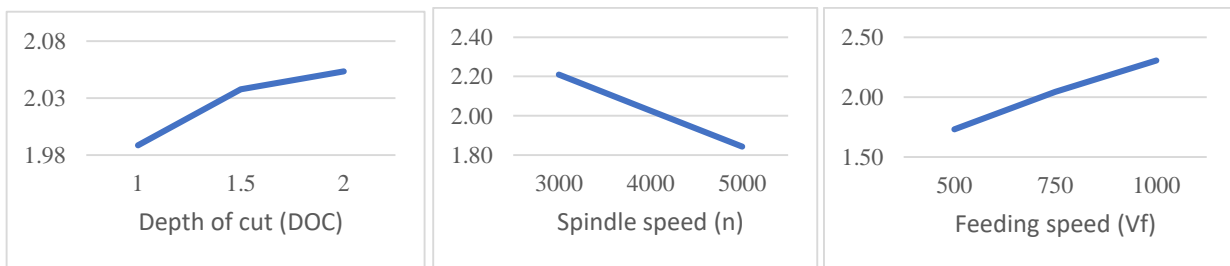
Fig.10 - The influence of process parameters on SR

6. Conclusions

In this study, the combination of firefly algorithm (FA) and back propagation neural network (BPNN) has shown to be able to minimize the cutting force (CF) and surface roughness (SR) in the end milling process of GFRP composite. The following points are the conclusions drawn from this study:

- The optimum BPNN topology of CF can be achieved using four hidden-layers, eight neurons in each hidden layer, logsig activation-function.
- The optimum BPNN topology of SR can be achieved using one hidden-layer, eight neurons in each hidden layer, as well as satlin activation-function.
- The BPNN has successfully predicted the minimum CF and SR after proper training is administered for the obtained average error value is less than 5%.
- The minimum value of CF and SR obtained through a combination of BPNN-FA for the input parameters have also been identified. The CF and SR responses can simultaneously be minimized by setting the depth of cut to be 1 mm, the spindle speed to be 4972 rpm, and the feeding speed to be 0.6475 mm/min.
- FA optimization method that is integrated with BPNN produces compelling results since all of the error value between the prediction and confirmation experiments is shown to be lower than 5%.

References

[1] Prasanth, I. S. N. V., Ravi Shankar, D. V. R., Hussain, M. M., Mouli, B. C., Sharma, V. K., & Pathak, S. (2018). Investigations on performance characteristics of GFRP composites in milling. The International Journal of Advanced Manufacturing Technology, 99, 1351–1360. https://doi.org/10.1007/s00170-018-2544-2

[2] Prasanth, I. S. N. V., Ravi Shankar, D. V. R., Hussain, M. M., & Mouli, B. C. (2017). Critical Analysis in Milling of GFRP Composites by Various End Mill Tools. Proceedings of the International Conference on Advanced Functional Materials, 14607-14617. https://doi.org/10.1016/j.matpr.2018.03.052

[3] Azmi, A. I., Lin, R. J. T., & Bhattacharyya, D. (2012). Experimental Study of Machinability of GFRP Composites by End Milling. Materials and Manufacturing Processes, 27, 1045–1050. https://doi.org/10.1080/10426914.2012.677917

[4] Azmi, A. I., Lin, R. J. T., & Bhattacharyya, D. (2013). Machinability study of glass fiber-reinforced polymer composites during end milling. The International Journal of Advanced Manufacturing Technology, 64, 247–261. https://doi.org/10.1007/s00170-012-4006-6

[5] Panneerselvam, K., Pradeep, K., & Asokan, P., (2012), Optimization of End Milling Parameters for Glass Fiber Reinforced Plastic (GFRP) Using Grey Relational Analysis. Procedia Engineering, 38, 3962-3968. https://doi.org/10.1016/j.proeng.2012.06.453

[6] Sreenivasulu, R. (2013) Optimization of Surface Roughness and Delamination Damage of GFRP Composite Material in End Milling Using Taguchi Design Method and Artificial Neural Network. Procedia Engineering, 64, 785-794. https://doi.org/10.1016/j.proeng.2013.09.154

[7] Çelik, Y. H., & Kılıçkap, E., & Yardımeden, A. (2014). Estimate of cutting forces and surface roughness in end milling of glass fiber reinforced plastic composites using fuzzy logic system. Science and Engineering of Composite Materials, 21(3), 435-443. http://dx.doi.org/10.1515/secm-2013-0129

[8] Jenarthanan, M. P., Gokulakrishnan, R., Jagannaath, B., & Raj, P. G. (2017). Multi-objective optimization in end milling of GFRP composites using Taguchi techniques with principal component analysis. Multidiscipline Modeling in Materials and Structures, 13(1), 58-70. https://doi.org/10.1108/MMMS-02-2016-0007

[9] Sharma, S., Chandrasekaran, M., & Thirumalai, R. (2014). Multi-objective optimization of surface roughness and tool wear in turning Inconel 718: A desirability analysis, genetic algorithm and firefly algorithm. Proceedings of the International Mechanical Engineering Congress, 545-549. https://doi.org/10.4028/www.scientific.net/AMM.592-594.545

[10] Senthilkumar, N., Tamizharasan, T., & Gobikannan, S. (2014). Application of Response Surface Methodology and Firefly Algorithm for Optimizing Multiple Responses in Turning AISI 1045 Steel, Arab J Sci Eng, 39, 8015–8030. http://dx.doi.org/10.1007/s13369-014-1320-3

[11] Lobato, F. S., Sousa, M. N., Silva, M. A., & Machado, A. R. (2014). Multi-objective optimization and bio-inspired methods applied to machinability of stainless steel Applied Soft Computing, 22, 261–271. http://dx.doi.org/10.1016/j.asoc.2014.05.004

[12] Raja, S. B., Pramod, C. V. S., Krishna, K. V., Ragunathan, A., & Vinesh, S. (2015). Optimization of electrical discharge machining parameters on hardened die steel using firefly algorithm. Engineering with Computers, 31, 1–9. http://dx.doi.org/10.1007/s00366-013-0320-3

[13] Shukla, R. & Singh, D. (2017). Selection of parameters for advanced machining processes using firefly algorithm. Engineering Science and Technology, an International Journal, 20, 212–221. http://dx.doi.org/10.1016/j.jestch.2016.06.001

[14] Gautam, G. D., & Mishra, D. R. (2019). Firefly algorithm based optimization of kerf quality characteristics in pulsed Nd:YAG laser cutting of basalt fiber reinforced composite. Composites Part B, 176, 107340 http://doi.org/10.1016/j.compositesb.2019.107340

[15] Rumelhart, D. E., Hinton, G. E., & Williams, R. J. (1986). Learning internal representations by error propagation, (pp. 318–362). Cambridge: MIT Press

[16] Soepangkat, B. O. P., Pramujati, B., Effendi, M. K., Norcahyo, R., & Mufarrih, A. M. Multi-objective optimization in drilling kevlar fiber reinforced polymer using grey fuzzy analysis and backpropagation neural network–genetic algorithm (BPNN–GA) Approaches. International Journal of Precision Engineering and Manufacturing 20(4), 593-607 https://doi.org/10.1007/s12541-019-00017-z

[17] X.S. Yang, (2008). Firefly algorithm. Nat. Ins. Meta. Algo, 20, 79–90

[18] Fister Jr., I., Yang, X. S., & Brest, J. (2013). A comprehensive review of firefly algorithms, Swarm and Evol. Comput., 13, 34–46. https://doi.org/10.1016/j.swevo.2013.06.001

[19] Park, K. H., Suhaimin, M. A., Yang, G. D., Lee, D. Y., Lee, S. W., & Kwon, P. (2017). Milling of Titanium Alloy with Cryogenic Cooling and Minimum Quantity Lubrication (MQL). The International Journal of Advanced Manufacturing Technology, 18, 5-14. https://doi.org/10.1007/s12541-017-0001-z

[20] Okafora, A. C., & Jasra, P. M. (2018). Effects of cooling strategies and tool coatings on cutting forces and tooth frequency in high-speed down-milling of Inconel-718 using helical bull-nose solid carbide end mills. The International Journal of Advanced Manufacturing Technology, 97, 2301-2318. https://doi.org/10.1007/s00170-018-2096-5

[21] Robbany, F., Pramujati, B., Suhardjono, Effendi, M. K., Soepangkat, B. O. P., & Norcahyo, R. (2019). Multi response prediction of cutting force and delamination in carbon fiber reinforced polymer using backpropagation neural network-genetic algorithm. AIP Conference Proceedings 2114, 030012. https://doi.org/10.1063/1.5112416.

[22] Fe-Perdomo, I. L., Beruvides, G., Quiza, R., Haber, R., & Rivas, M. (2018). Automatic Selection of Optimal Parameters Based on Simple Soft-Computing Methods: A Case Study of Micro milling Processes. IEEE Transactions on Industrial Informatics, 15(2), 800-811. https://doi.org/10.1109/TII.2018.2816971

[23] Davim, J. P., Reis, P., & Conceicao, A. C. (2004). A study on milling of glass fiber reinforced plastics manufactured by hand-lay up using statistical analysis (ANOVA). Composite Structures, 64, 493–500. https://doi.org/10.1016/j.compstruct.2003.09.054

[24] Davim, J. P., & Reis, P. (2005). Damage and dimensional precision on milling carbon fiber-reinforced plastics using design experiments. Journal of Materials Processing Technology, 160, 160–167. https://doi.org/10.1016/j.jmatprotec.2004.06.003

[25] Razfar, M. R., & Zadeh, M. R. Z. (2009). Optimum damage and surface roughness prediction in end milling glass fibre-reinforced plastics, using neural network and genetic algorithm. Proceedings of the Institution of Mechanical Engineers Part B: Journal of Engineering Manufacture, 223, 653-664. https://doi.org/0.1243/09544054JEM1409

[26] Jenarthanan, M. P., & Jeyapaul, R. (2013) Optimisation of machining parameters on milling of GFRP composites by desirability function analysis using Taguchi method. International Journal of Engineering, Science and Technology, 5(4), 23-36, http://dx.doi.org/10.4314/ijest.v5i4.3

[27] Stephensen, D. A., & Agapiou, J. S. (2006). Metal Cutting Theory and Practice. 2nd ed. CRC Press. Taylor & Francis Group, L.L.C

[28] Raj, P. R., Perumal, A E., & Ramua, P. (2012). Prediction of surface roughness and delamination in end milling of GFRP using mathematical model and ANN. Indian Journal of Engineering & Materials Sciences, 19, 107-120